TURBULENT BURNING MODEL FOR PREMIXED GASEOUS MIXTURES

E. M. J. Mushi
Mechanical Engineering Department,University of Dar es Salaam
P.O. Box 35131, Dar es salaam, Tanzania
E-mail:ejmushi@hotmail.com

Abstract

A turbulent burning model for premixed gaseous mixtures has been successfully developed. The model assumes instant burning of vortex tubes of the order of Kolmogorov scale followed by burning of larger eddies of the order of Taylor micro scale. These eddies burn at a rate dependent on the stretch rate. The influence of turbulence on the burning rate is introduced in the form of probability density function which gives the probability that a given mixture under turbulence will undergo burning rather than being quenched. The model has been validated against experiments involving turbulent explosions in a fan stirred bomb. Model predictions were in good agreement with experiments.

Introduction

When a turbulent flame is photographed as it propagates outwards from a point source it has the appearance of a fireball. A laser sheet photograph, gives a different picture, indicating that at higher turbulence levels there is appreciable unburnt gas behind the flame front that is indicated by conventional self-luminous and schlieren photographs. This is in agreement with the Tennekes [1] model of small scale structure of turbulence which suggested that the small scale structure of turbulence may be modeled as vortex tubes of diameter η, (the Kolmogorov micro-scale), which are stretched by eddies of size λ, (the Taylor micro-scale). This model implies that dissipative eddies consist of a random agglomeration of vortex tubes with a diameter of the order of the Kolmogorov scale, η, and a spacing of the order of the Taylor micro scale, λ. Experimental support for this model is provided by the works of Kuo and Corrsin [2,3].

The stretching of the vortices is the means by which these gain kinetic energy from the larger sizes. In the small length scales that are associated with these vortices the energy is converted finally into thermal internal energy via viscous

dissipation. Molecular mixing also occurs in these scales (of the order of the Kolmogorov scale). This and the increased gas temperature can then relieve the stretch on these scales to create conditions favorable for accelerated flame propagation. Experimental[4] and theoretical work [5,6] suggest flame propagation speeds, along a vortex tube, to be higher than laminar speeds.

The model presented in this work assumes that the mass rate of burning behind schlieren front is proportional to the mass of unburned mixture behind it. The constant of proportionality is a reciprocal time constant. Such a formulation originally was proposed by Blizard and Keck[7] and later modified by Tabaczyski et al.[8] and Daneshyar et al.[6] . These earlier formulations were observed to provide inadequate predictions even in the conditions for which they were developed. These were developed for internal combustion engines in which the turbulence level is limited during the combustion process. In this way it was not necessary to account for the influence of the turbulence on the process of combustion. Further the flame entrainment velocity was considered to be a slowly varying parameter with respect to turbulence. It has been shown[9], that the entrainment velocity varies considerably with turbulence and increases with time elapsed since ignition. Another weakness of the earlier models is that they did not account for flame stretch arising from the turbulence which is known to affect considerably the burning rate. Excessive flame stretch is known to quench flames. In addition since the models were based on limited turbulence level, they could not be applied generally to give predictions at different turbulence levels. The present model is an attempt to address these limitations.

Eddies are considered to be entrained at the flame front at an entrainment velocity which was a slowly varying parameter on the time scale of the combustion process. In what was essentially a laminar flamelet model these eddies subsequently burned behind the front in a characteristic time, given by the eddy radius divided by the laminar burning velocity. It followed from these assumptions that the amount that remained unreacted decayed exponentially with time.

Ignition is assumed to occur across the highly dissipative region of the order of the Kolmogorov scale[8] and the burning in this region is instantaneous. Further the burn-up of the mixture situated between the highly dissipative regions is governed by the spacing, λ, and the laminar burn-up across that space. In addition

the rate of burning is assumed to be proportional to the mass of unburned gas behind the flame front. The constant of proportionality is a reciprocal of a time constant.

In the present model a spherical turbulent flame propagating from a point source at constant pressure is analyzed. The burning velocity is considered to develop with time and this is included in the model, along with its dependency upon flame stretch and the ratio u_k'/u_l. Correlations of turbulent burning velocity in terms of the theoretically appropriate dimensionless groups[10,11] are used to establish the entrainment velocity.

To account for the influence of turbulence a flame spreading from a point source, is considered to be initially smaller than most of length scales of turbulence and its propagation time is smaller than most of the time scales of turbulence. Turbulent velocities act as convection velocities on the kernel which propagates relative to the unburnt gas at the laminar burning velocity[12]. As the kernel grows it first becomes affected by the highest frequencies of the turbulence spectrum. The lower frequencies become increasingly influential with flame growth. The effective r.m.s velocity experienced by the flame, u_k', increases with the increase in the influential range of the turbulent spectrum and it ultimately attains its maximum value, equal to the fully developed turbulent r.m.s velocity, u', when the full spectrum is embraced.

The development of the turbulent burning velocity, u_{tk}, associated with u_k', is related to the temporal development of the latter[9] equation (1),

$$\frac{u_t(\bar{t})}{u'} = \left(\frac{u_t}{u_l}\right)\left(\frac{u_l}{u'}\right)\left[1-\exp(-0.2(\frac{t}{\tau_a})^{0.75})\right]^{0.5} \qquad (1)$$

where, $\tau_a = L/u'$. The value of u_t/u_l, the fully developed turbulent velocity ratio, is obtained from the correlations of turbulent burning velocity [11] by considering u_k'/u_l to be equal to u'/u_l. During the early laminar burning, the rate of entrainment is assumed equal to the laminar burning velocity.

Stretching of a flame occurs when there is a component of gas velocity along the flame front. Wrinkling of the flame increases the turbulent burning velocity by virtue of the increased area presented by the wrinkled laminar flame. However,

eventually, excessive flame stretch can locally extinguish a laminar flamelet. Throughout the present work it is assumed that a turbulent flame consists of an array of laminar flamelets.

In turbulent flow the stretch rate derived from aerodynamic strain rate is not single valued but distributed[11]. This distribution of stretch rates means that different parts of a flamelet experience different stretch rates. Depending on the magnitudes of these rates, parts of the flame may suffer quenching, while others propagate. Premixed laminar flames have a well defined limiting stretch rate at which the flame quenches[14,15]. If the stretch rate at which the flame quenches is known, the propagating parts of a flame must have stretch rates less than this quenching value. In the present work the proportion of the entrained unburned mass which is capable of undergoing burning is assumed equal to the probability, p(b), that the stretch rate acting on a potential flame is less than the quenching value, s_{qt}. It is further assumed that the laminar burning velocity is unchanged up to a stretch rate of s_{qt} and that above this value it falls to zero.

The probabiility p(b) is evaluated using equation (2) for $\kappa_{qt}Le > \kappa'Le$ and equation (3) for $\kappa_{qt}Le \leq \kappa'Le$[11,13].

$$p(b) = 0.5\left[1+erf\left(\frac{\kappa_{qt}Le-\kappa'Le}{\sqrt{2}\sigma_k Le}\right)\right] \qquad (2)$$

$$p(b) = 0.5\left[1+erf\left(\frac{\kappa'Le-\kappa_{qt}Le}{\sqrt{2}\sigma_k Le}\right)\right] \qquad (3)$$

The error function is given by equation (4) while the value of κ'Le is evaluated using equation (5).

$$erf(y) = \frac{2}{\sqrt{\Pi}}\int_0^y e^{-x^2}dx \qquad (4)$$

$$\kappa'Le = 1.08(KLe)e^{-a/KLe} \qquad (5)$$

Finally the value of σ_kLe is established using equation (6).

$$\sigma_k Le = \left[1+0.32e^{-a/KLe}\right]KLe \qquad (6)$$

with, a, the constant value of a stretch dependency factor, equal to 0.0132. The turbulent quenching stretch rate is best related to KLe by equation (7)[11]

$$\kappa_{qt}Le = 0.166 - 0.014KLe \tag{7}$$

The turbulent mass burning rate is expressed as the rate of decrease of unburned mass behind the flame front[8]. It is assumed to be proportional to the unburned mass of mixture behind the front, m_u . In addition, allowance for flame quenching is introduced by making this rate also proportional to the probability, p(b).

$$\frac{dm_u}{dt} = \frac{-m_u p(b)}{\tau} \tag{8}$$

For generality the reciprocal time constant, τ, is defined by equation (9) where c is a constant related to the geometry of the burning across the Taylor scale. This constant is to be determined through experiments.

$$\tau = \frac{c\lambda}{u_l} \tag{9}$$

The ratio of the effective aerodynamic strain rate to the fully developed value, for a flame propagating from a point source, is correlated with the dimensionless time, t/τ_a [10]. The proposed variation, suggests the fully developed value to be attained at dimensionless time close to 0.1. During the early stages, in addition to flame stretching due to the aerodynamic strain, a geometrical stretch (=(2/r)dr/dt), where r is the flame radius, also acts upon the flame. With spark ignition the dimensionless duration of 0.1 is usually close to the discharge time. In this early stage burning is laminar, with a possible enhancement of the normal value of u_l due to electrical discharge. During this early stage the turbulent velocity acts as convective velocity on the small flame kernel and any flame wrinkling arises from the higher frequency components of the turbulence as flame stretching begins to develop. At this time flame propagation has not developed and the proposed burning model is not applicable. Once the strain rate, at $\bar{t}$=0.1, is fully developed, with some validity, it may be assumed that p(b) is constant, as well as τ, and that the proposed turbulent burning model is applicable.

Furthermore, it is assumed that the effect of geometrical stretch on the propagation of the flame speed is negligible after this time. Although, in practice, flame stretch decreases the value of u_l, here it is assumed that$_l$ u retains its unstretched value for all stretch rates less than the quenching value, s_{qt}, then it

decreases, step-wise, to zero at stretch rates greater than this. This is reflected in the value of p(b). In the present model it is assumed that the full stretch rate develops instantaneously when $\bar{t}$=0.1. Up to this time flame propagation is assumed to be laminar. After it turbulent entrainment and burning dominates. For the initial laminar combustion at time t' after the start of combustion from a point source the rate of change of burned mass is given by equation (10).

$$\frac{dm_b(t')}{dt'} = A_f(t')u_l\rho_u \qquad (10)$$

This neglects the effect of geometric flame stretching or assumes it is countered by a spark energy in excess of the minimum ignition energy. If this mode of burning continues to time t_l, the total mass burned at that time is given by equation (11).

$$\int_{t'=0}^{t'=t_l} dm_b(t') = m_b(t_l) = \rho_u \int_{t'=0}^{t'=t_l} A_f(t')u_l dt' \qquad (11)$$

After time t_l burning is assumed to be in the entrainment mode. For a mass entrained by the flame front at time t', integration of equation(8) gives the amount remaining unburned at a later time, t

$$\int_{m_{u(t')}}^{m_{u(t)}} \frac{dm_u}{m_u} = \frac{-p(b)}{\tau}\int_{t'}^{t} dt \qquad (12)$$

It follows that

$$m_u(t) = m_u(t')\exp\left[\frac{-p(b)(t-t')}{\tau}\right] \qquad (13)$$

Of the original mass entrained at time t', $m_u(t')$, the mass burned, during this time, $m_b(t)$, is the difference between the initial mass unburned at time t' and that which remains unburned at time t, equation 14.

$$m_b(t) = m_u(t')\left(1-\exp\left[\frac{-p(b)(t-t')}{\tau}\right]\right) \qquad (14)$$

The rate of entrainment of mass, m_e, at any time t' is related to the mean flame area, $A_f(t')$, and the turbulent burning velocity at that instant, $u_t(t')$, as well as the

density of the unburned gas, ρ_u, assumed to be constant, by:

$$\frac{dm_e(t')}{dt'} = A_f(t')u_t(t')\rho_u \tag{15}$$

Of the mass $dm_e(t')$ entrained at time t' in the time interval dt', the amount burnt at a later time, t, is, from equations (14) and (15) :

$$dm_b(t-t') = A_f(t')u_t(t')\rho_u dt'[1-\exp(-p(b)(t-t')/\tau)] \tag{16}$$

To find the total amount burnt at time t, account must be taken of all the amounts of unburnt gas entrained at different values of t'. This extends over a range of t' from t_l to t. Hence

$$lm_b(t-t') = m_b(t) = \rho_u \int_{t'=t_l}^{t'=t} A_f(t')u_t(t')[1-\exp(\frac{-p(b)(t-t')}{\tau}) \tag{17}$$

The total mass entrained by the flame, at time t, from equation (15) is given by equation (18)

$$m_{e(t)} = \rho_u \int_{t'=0}^{t'=t} A_f(t')u_t(t')dt' \tag{18}$$

By equating the rate of dissipation of turbulent energy to the rate of decay of the energy containing eddies, of average size l_e,[16], equation 19 is obtained.

$$\frac{\lambda^2}{l_e} \propto \frac{\nu}{u'}. \tag{19}$$

Assuming a linear relation between l_e and L, [9], the Taylor scale is related the to the integral length scale, by equation (20) :

$$\frac{\lambda^2}{L} = \frac{40.4\nu}{u'} \tag{20}$$

This gives equation (21), and from equations. (9) and (20), equation (22) is obtained for the constant of proportionality, τ.

$$\lambda = \sqrt{40.4LR_L^{-0.5}} \tag{21}$$

$$\tau = c\frac{\sqrt{40.4LR_L^{-0.5}}}{u_l} \tag{22}$$

Equation (22) substituted into equation (17) and together with equation (11), give the total mass burned behind the flame front at time t from both stages of combustion, equation (23).

$$\begin{aligned} m_b(t) = \rho_u \int_{t'=t_l}^{t'=t} A_f(t')u_t(t')[1-\exp(\frac{-p(b)(t-t')u_l}{c\sqrt{40.4}LR_L^{-0.5}})]dt' \\ + \rho_u \int_{t'=0}^{t'=t_l} A_f(t')u_l dt' \end{aligned} \tag{23}$$

For a flame propagating from a point source the mean flame area, is dependent on the time dependent turbulent burning velocity, u_t, and the mass behind the front. This dependency cannot be approximated as a function of time, and hence an analytical solution of the mass burned equation is not possible and recourse must be made to numerical solutions. For this, the relation between the flame area and the total burned and unburned mass is essential.

In order to attain the greatest possible generality of the numerical solutions, the governing equations should be dimensionless. Equation (23) in dimensionless terms becomes:

$$\begin{aligned} M_b(\bar{t}) = \int_{\bar{t}'=\bar{t}_l}^{\bar{t}'=\bar{t}} \bar{A}_f(\bar{t})\frac{u_t(\bar{t}')}{u'}[1-\exp(-p(b)(\bar{t}-\bar{t}')/(cB))]d\bar{t}' \\ + \int_{\bar{t}'=0}^{\bar{t}'=\bar{t}_l} \frac{\bar{A}_f(\bar{t}')u_l}{u'}d\bar{t}' \end{aligned} \tag{24}$$

and

$$M_e(\bar{t}) = \int_{\bar{t}'=0}^{\bar{t}'=\bar{t}} \frac{\bar{A}_f(\bar{t}')u_t(\bar{t}')}{u'}d\bar{t}' \tag{25}$$

Equation 26 gives the dimensionless Karlovitz flame stretch factor for isotropic

turbulence[17]. From this expression the variable B can be expressed in terms of KLe, Le and u'/u_l equation (27).

$$K=0.157(u'/u_l)^2 R_L^{-0.5} \tag{26}$$

$$B=\frac{\sqrt{40.4}KLe}{0.157Le(u'/u_l)} \tag{27}$$

Equations (24) and (25) give the total mass burned and the total entrained during the two stages of combustion. A flame must be initiated by a small amount of burnt gas and this is given by $M_b(\bar{t}=0)$. It follows that :

$$M_b(\bar{t})=\int_{\bar{t}'=\bar{t}_i}^{\bar{t}'=\bar{t}} \bar{A}_f(\bar{t})\frac{u_t(\bar{t}')}{u'}[1-\exp(-p(b)(\bar{t}-\bar{t}')/(cB))]d\bar{t}' + \int_{\bar{t}'=0}^{\bar{t}'=\bar{t}_i} \frac{\bar{A}_f(\bar{t}')u_l}{u'}d\bar{t}' + M_b(\bar{t}'=0) \tag{28}$$

$$M_e(\bar{t})=\int_{\bar{t}'=0}^{\bar{t}'=\bar{t}} \frac{\bar{A}_f(\bar{t}')u_t(\bar{t}')}{u'}d\bar{t}' + M_b(\bar{t}'=0) \tag{29}$$

The initial mass is assumed to be completely burned at the adiabatic burnt gas density and to occupy a sphere.

Flame radius and area

Increasing turbulence changes the flame surface from smooth to wrinkled and finally to fragmented. Inevitably an equivalent smooth surface must be defined to be associated with the burning velocity. In practice this area is highly dependent on the enclosing chamber. However, experiments have shown that the developing flame is near-spherical when its size is small compared to the dimensions of the chamber. From this point in the analysis spherical flames will be assumed.

A further assumption is made that the mass behind the flame front consists of burnt gas at the adiabatic, completely burnt density, ρ_b, and unburned gas at the initial density, ρ_u. If the flame radius is $r(t)$, it can be defined in terms of the volume occupied by the unburnt and burnt gas :

$$\frac{4}{3}\pi(r_f(t))^3 = \frac{m_u(t)}{\rho_u} + \frac{m_b(t)}{\rho_b} \tag{30}$$

Because the unburned mass is equal to the difference between the entrained and the burned mass, $m_u(t) = m_e(t) - m_b(t)$, the above equation can be rearranged to give the flame radius :

$$r_f(t) = \{\frac{3}{4\pi\rho_u}[m_e(t) + m_b(t)(\frac{\rho_u}{\rho_b} - 1)]\}^{\frac{1}{3}} \tag{31}$$

The spherical flame area is obtained from this radius :

$$A_f(t) = (4\pi)^{\frac{1}{3}}\{\frac{3}{\rho_u}[m_e(t) + m_b(t)(\frac{\rho_u}{\rho_b} - 1)]\}^{\frac{2}{3}} \tag{32}$$

In dimensionless form equations. (36) and (37) become :

$$\bar{r}_f(t) = \{\frac{3}{4\pi}[M_e(\bar{t}) + M_b(\bar{t})(\frac{\rho_u}{\rho_b} - 1)]\}^{\frac{1}{3}} \tag{33}$$

$$\bar{A}_f(\bar{t}) = (4\pi)^{\frac{1}{3}}\{3[M_e(\bar{t}) + M_b(\bar{t})(\frac{\rho_u}{\rho_b} - 1)]\}^{\frac{1}{3}} \tag{34}$$

Numerical method

In the numerical solution the region behind the flame front comprises a series of elemental masses within concentric spherical shells (only spherical flames are considered in this work). Each shell contains the dimensionless mass entrained during an interval of one constant dimensionless time step, $\Delta\bar{t}$. The elemental shells are numbered consecutively, such that the one element containing the mass entrained during the first time increment is number one and that for the last element is n. The sum of the masses entrained in each element gives the total mass entrained at a given time. The mass burned in each element is evaluated for the time since entrainment and the last entrained element is completely unburned. The ratio of mass burned to mass entrained in each element increases towards the center of the flame. The summation of the elemental burnt masses gives the total mass burned at the elapsed time.

The flame radius and area are evaluated from the total mass entrained and the total mass burned, equations (33) and (34). To do this the finite difference forms of

$$\frac{u_t(\bar{t}_i)}{u'} = \frac{u_t}{u_l}\frac{u_l}{u'}\{1-\exp(-0.2(\bar{t}'(i))^{0.75})\}^{0.5} \quad (35)$$

some of the equations are required as indicated equations 35 to 40. Equation 35 drives the flame front forward where $\bar{t}'(I)$ is a general intermediate time. The value of u_t/u_l is obtained from the correlations by Bradley et al[11].

$$M_e(\bar{l}(n)) = \sum_{i=1}^{n} \bar{A}_f(\bar{t}'(i-1))\frac{u_t(\bar{t}'(i))}{u'}\Delta\bar{t}' + M_e(\bar{t}'=0) \quad (36)$$

$$M_b(\bar{l}(n)) = \sum_{i=n_l+1}^{n} \bar{A}_f(\bar{t}'(i-1))\frac{u_t(\bar{t}'(i))}{u'}[1-\exp(\frac{-p(b)(\bar{l}(n)-\bar{t}'(i))}{cB})]\Delta\bar{t}' + \sum_{i=1}^{n_l} \bar{A}_f(\bar{t}'(i-1))\frac{u_l}{u'}\Delta\bar{t}' + M_b(\bar{t}'=0) \quad (37)$$

$$\dot{r}_f(\bar{l}(n)) = \{\frac{3}{4\pi}[M_e(\bar{l}(n)) + M_b(\bar{l}(n))(\frac{\rho_u}{\rho_b}-1)]\}^{\frac{1}{3}} \quad (38)$$

$$\bar{A}_f(\bar{l}(n)) = (4\pi)^{\frac{1}{3}}\{3[M_e(\bar{l}(n))+M_b(\bar{l}(n))(\frac{\rho_u}{\rho_b}-1)]\}^{\frac{2}{3}} \quad (39)$$

Here n is the total number of elements entrained at time $\bar{t}(n)$, I the element number and n_l is the element number at which laminar burning ceases. The total mass entrained and burned at time $\bar{t}=0$ is given by equation 40.

$$M_e(\bar{t}=0) = M_b(\bar{t}=0) = \frac{4}{3}\pi(\rho_b/\rho_u)\dot{r}_f^3(\bar{t}=0) \quad (40)$$

The computational cycle

The computational cycle is starts by assigning values to u',u_l, Kle, Le and the expansion ratio ρ_u/ρ_b. The value of u_t/u is obtained from the correlations developed by Bradley et al [11].

This is followed by evaluation of κLe, σ_κLe, κ_{qt}Le, B and p(b) from equations (7-9,29,4 or 5) respectively. To complete the calculation for the parameters which will remain constant throughout one solution, the initial total mass burned, which is equal to the total mass entrained at that time is evaluated from equation (42) and the given value of $\dot{r}_f(\bar{t}=0)$. The initial flame area, is then evaluated from equation

(36) followed the value of the initial mass entrained and burned.

The solution loop starts by incrementing the time $\bar{t}$ by one time step $\Delta\bar{t}$' and the element counter n by 1. If the loop is being implemented for the first time the time and the counter are all equal to 0 before this increment. This is followed by a selection of the equation to be used for the evaluation of the ratio of time dependent turbulent burning velocity to the turbulent r.m.s velocity, $u_t(\bar{t}(n))/u'$. If the dimensionless time is less or equal to 0.1 then laminar burning predominates and $u_t(\bar{t}(n))/u' = u_l/u'$. Where $\bar{t} > 0.1$ equation (37) is used. The next step evaluates the mass entrained in each element and sums these to give the total mass entrained up to the time, $M_e(\bar{t}(n))$, equation (38). This is followed by calculation of the mass burned in each element, the sum of which gives the total mass burned, $M_b(\bar{t}(n))$, equation (39).

The new flame dimensionless flame radius and area are then calculated from the total mass entrained and the total mass burned using equations (40) and (41). This marks the end of the calculation loop which is repeated with an additional time increment until the required time has elapsed.

The time increment was established from three initial guesses. These were selected such that each was half the previous one. The mean square deviation of computed results between the first and second choices, and the second and the third choices were evaluated. On the assumption of a linear relationship between the mean deviation and the time increment, the increment for zero deviation was calculated. This became the third guess and the procedure was repeated. A relative error, $\epsilon \leq 10^{-4}$ was used as a convergence criterion. This was defined as :

$$\epsilon = \frac{\Delta\bar{t}_3 - \Delta\bar{t}_2}{\Delta\bar{t}_3} \qquad (41)$$

The appropriate time step was taken to be equal to the third guess when the convergence criterion was satisfied. From this procedure a time step $\Delta\bar{t} = 0.01$ was found to satisfy the criterion for all the conditions covered in this analysis and, consequently, this was used throughout.

The constant c was obtained from best fits of experimental data. A value of c = 0.28 gave the best fits and was used for all the results presented in this work.

Daneshyar and Hill[16] recommend an initial flame radius of 2 mm for use in spark ignition engines. Experimental[18] and theoretical[20], suggest that the kernel radius of a spark ignited mixture reaches 2.0 mm in less than 0.1 ms. From this, an initial flame radius of 2 mm was assumed for the analysis. The length scale, L, varies with turbulence and the dimensions of the combustion chamber. In the experiments reported in this work the integral length scale varied from 20 to 50 mm, and it was found that an initial dimensionless radius of $\dot{r}_f(\bar{t}=0)=0.04$ gave a good fit between theoretical and experimental data. This value therefore was adopted in all the computations.

Experiments

The experiments used in this work were conducted in a fan stirred bomb, comprising a cylinder of 305 mm diameter and 300 mm length, with 150 mm diameter concentric windows on each end plate. These windows provided optical access for schlieren photography and emission measurements. The arrangement is shown on fig. 1.

Flame propagation was recorded using schlieren photography with a high speed cine camera. Projected flame images were digitised and scaled to reflect actual flame sizes. The radius of a circle having an enclosed area equal to that of the

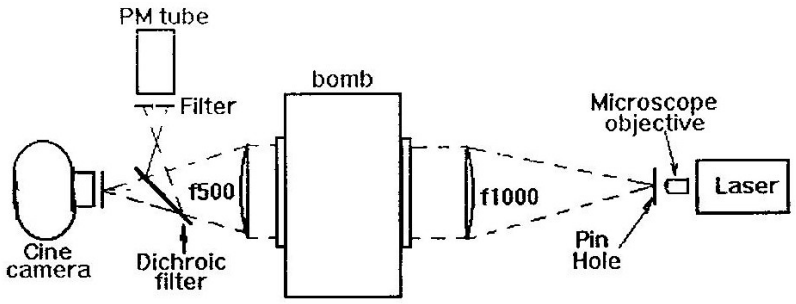

Fig. 1 Schlieren and CH measurements

projected image was evaluated and considered the equivalent flame radius. Timing

marks provided on the film by the camera facilitated the evaluation of the corresponding time after ignition for each image. The two gave a time radius data for the flame. A capacitor discharge ignition system with two identical electrodes was used to ignite mixtures of methane and air at centre of the combustion vessel. Details of the arrangement and experimental procedures are discussed elsewhere [18, 21,22].

The intensity of chemiluminescent emissions from the CH radicals formed in the flame reaction zone are proportional to the volumetric rate of consumption of combustible mixture[18,23]. An important characteristic of the intensity is that, as it represents the volumetric rate of consumption of fresh mixture, the ratio of intensities from two flames of same radius will represent the ratio of their mass burning velocity. Laminar flames were used for comparison thus giving the ratio of turbulent mass burning velocity, u_{tr}, to the laminar burning velocity, u_l.

In addition the dimensionless mass burning velocity was evaluated from the experimental values of the flame speed S, the laminar burning velocity, u_l, the fully developed turbulent velocity, u_t, evaluated using correlations, and the adiabatic expansion ratio, ρ_u/ρ_b, Equation 42[10]

$$\frac{u_{tr}}{u_l} = \frac{S-u_t}{u_l\left(\rho_u/\rho_b-1\right)} \qquad (42)$$

Comparison of model predictions with experiments

The model was run to simulate the different experimentally observed flame kernel growth and the measured burning velocity ratio. The after-burning time constant, τ ($=c\lambda/u_l$) in the model, embodies the unburned constant c, which required evaluation. Large value of c results in a low burning rate and a slow kernel growth rate. Measured flame kernel radii were compared with those theoretically predicted for different values of c.

Each set of initial conditions was calibrated by adjusting the constant c until the best fit to the experimentally determined data was achieved. The experiments were conducted at atmospheric pressure and at a temperature of 328 K. An initial dimensionless radius of 0.04 was used in the model. Further information on the conditions is given in Table 1.

Laminar burning velocities were obtained from Andrew and Bradley[20] and Le from Abdel-Gayed et al.[24] and Al-Khishali[25]. Values of ρ_u/ρ_b were obtained from an algorithm by Habik[26]. Comparisons of experimental flame radius to model predictions are shown in Figs. 2 to 7. In addition, prediction of the dimensionless mass burning velocity is compared to that measured using CH emissions and that evaluated using equation 42 for similar conditions on Figs. 8 to 13. Best fits were obtained with a value of $c=0.28\pm0.02$ for all the experiments.

Table 1 Conditions for comparison of predictions to experiments

Figures	θ	Le	u_l m/s	ρ_u/ρ_b	u' m/s
2,8	0.83	1.012	0.32	6.29	1.73
3,9	0.91	1.012	0.38	6.61	
4,10	1.00	1.049	0.43	6.88	
5,11	1.10	1.088	0.45	6.93	
6,12	1.00	1.049	0.43	6.88	3.0
7,13	1.00	1.049	0.43	6.88	6.0

Generally model predictions are in good agreement with experiments for a value of $c=0.28$. Figures 2 to 7 indicate very good predictions of the flame radius as the flame develops with time for different equivalence ratios and r.m.s turbulent velocity. For the dimensionless mass burning rate, Fig. 8 to 13, the experimental values indicate considerable fluctuations. This are to be expected given the nature of interaction between geometrical and aerodynamic stretch on one hand and the flame. This may be associated with the distribution of stretch rates. Compared to the experimental data, the model gives values which are representative of the mean values of the dimensionless mass burning rate.

It follows from this that the value of c is independent of equivalence ratio within the range 0.83 to 1.1. It is also independent of turbulence for r.m.s turbulent velocity between 1.73 and 6 m/s.

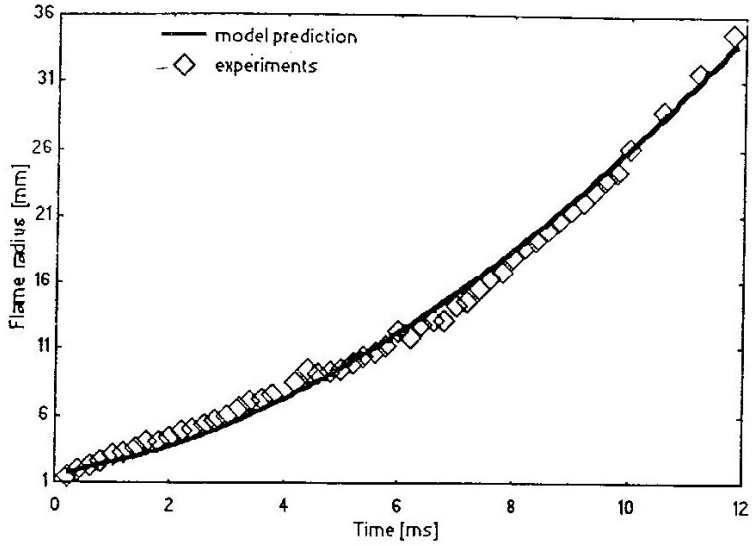

Fig. 2 Flame radius vs time
u'=1.73 m/s θ=0.83

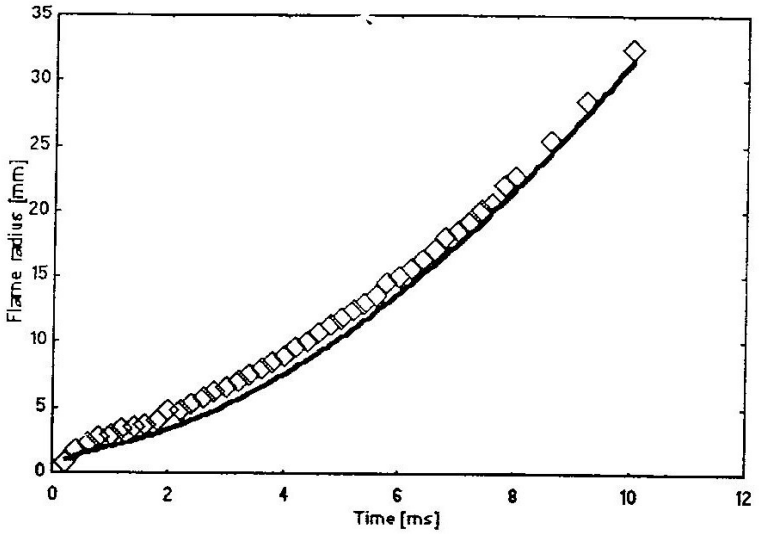

Fig. 3 Flame radius vs time
u'=1.73 m/s θ=0.98

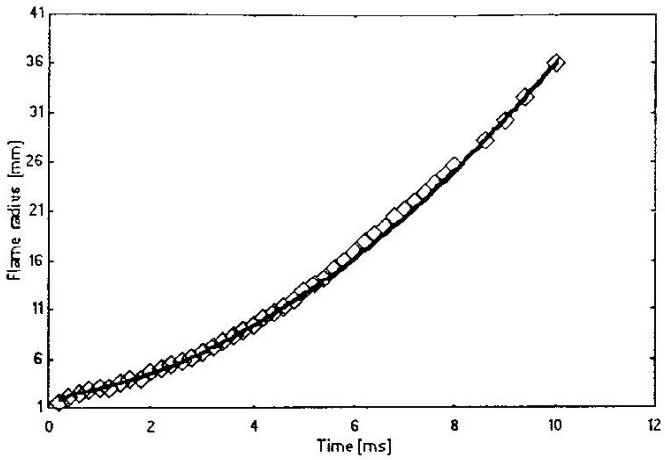

Fig. 4 Flame radius vs time
u'=1.73 m/s θ=1.0

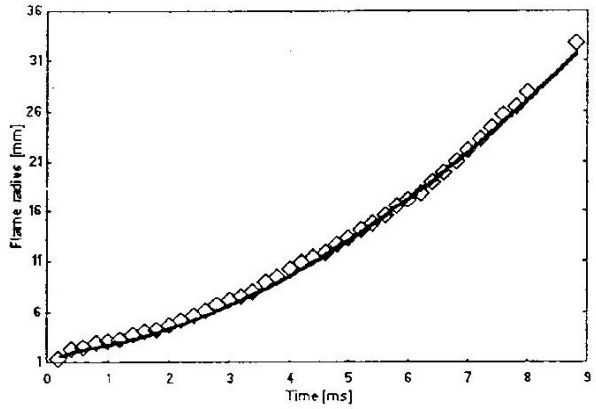

Fig. 5 Flame radius vs time
u'=1.73 m/s θ=1.1

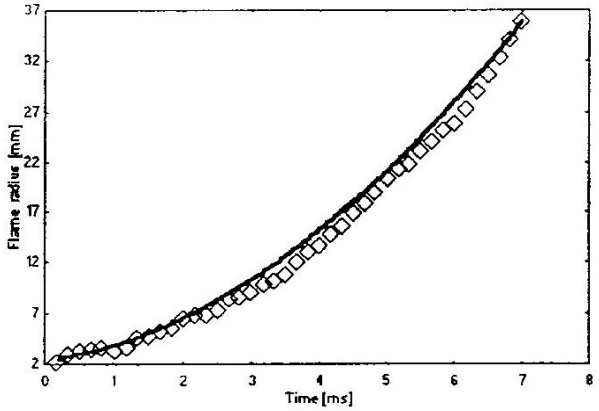

Fig. 6 Flame radius vs time
u'=3.0 m/s θ=1.0

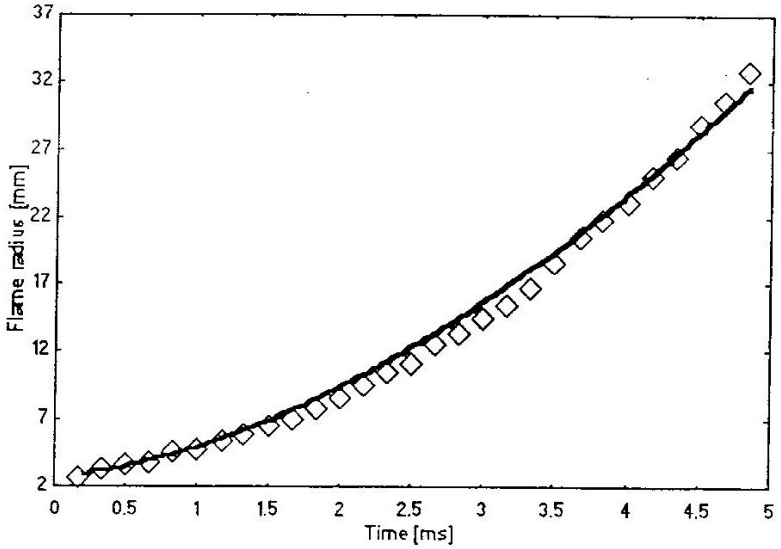

Fig. 7 Flame radius vs time
u'=6.0 m/s θ=1.0

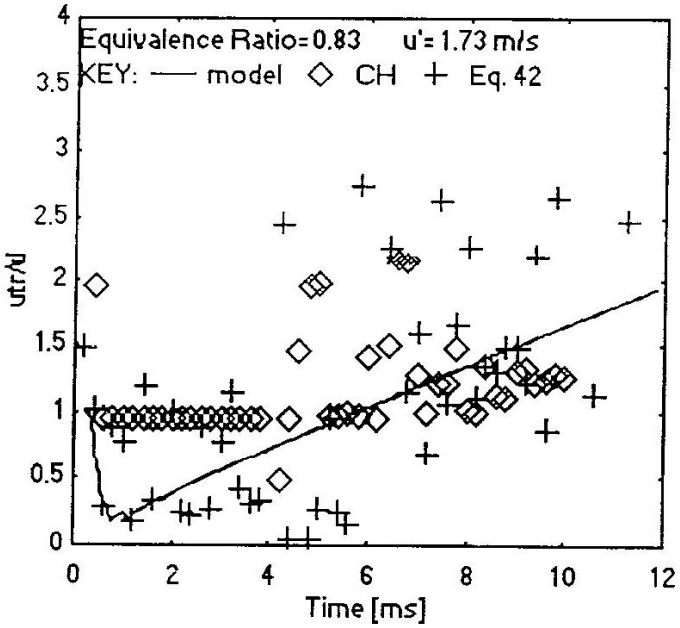

Fig. 8 Dimensionless mass burning rate
vs time (θ=0.83, u'=1.73 m /s

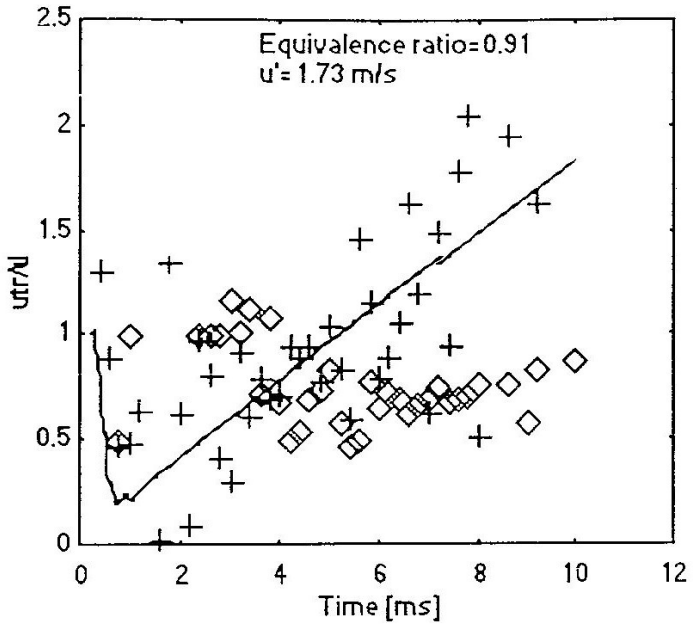

Fig. 9 Dimensionless mass burning rate vs time (θ=0.9 u'=1.73 m/s)

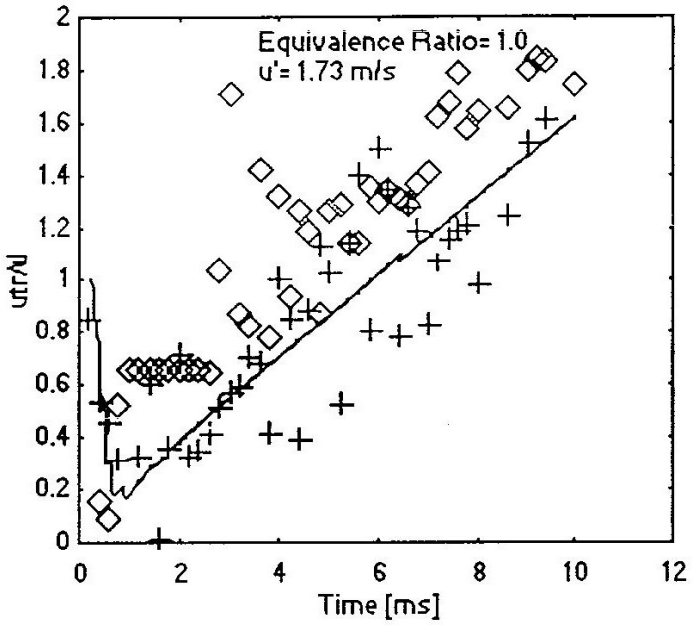

Fig. 10 Dimensionless mass burning rate vs time (θ=1.0 u'=1.73 m/s)

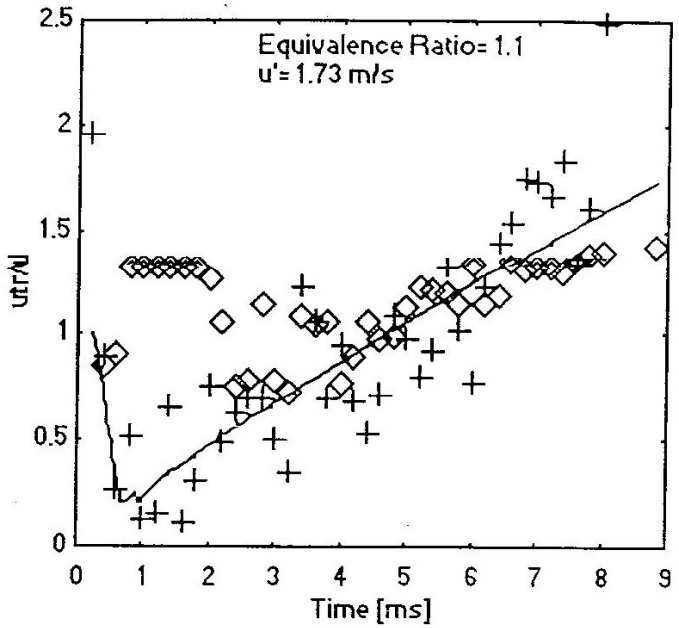

Fig. 11 Dimensionless mass burning rate vs time (θ=1.1 u'=1.73)

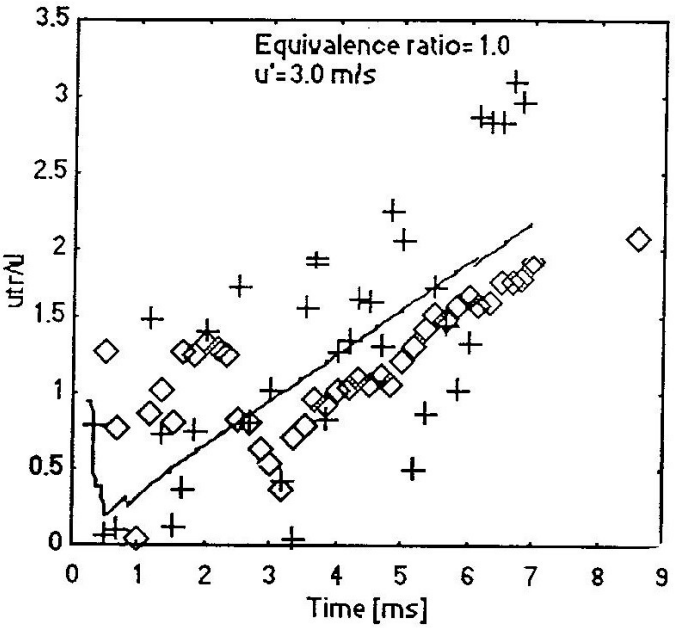

Fig. 12 Dimensionless mass burning rate vs time (θ=1.0, u'=3.0 m/s)

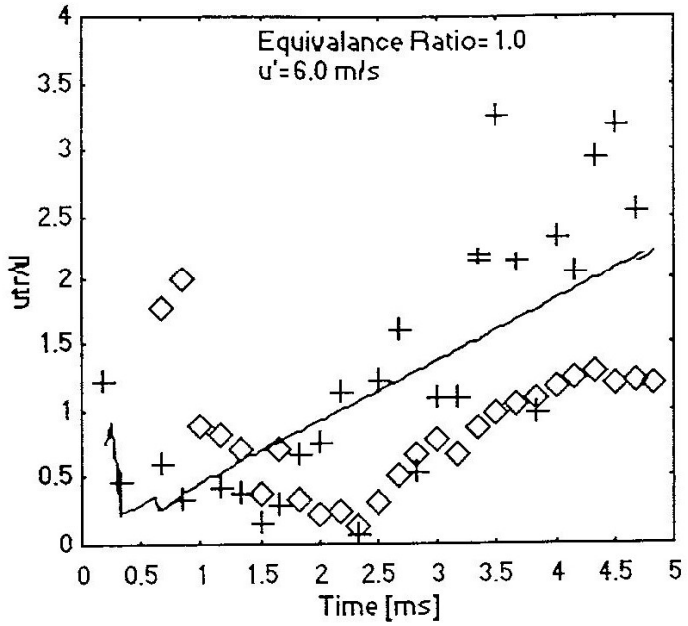

Fig. 13 Dimensionless mass burning rate Vs time (θ=1.0, u'=6.0 m/s

CONCLUSION

A turbulent entrainment and after-burning model has been successfully developed. This is based upon the latest available data on turbulent burning velocity. This model does include the effects of flame stretch.

The model has been validated against experiments involving turbulent explosions in a fan-stirred bomb and a consistent value of the time constant, $c=0.28(\pm 0.02)\lambda/u_l$, found to give good approximations to the experimental values.

An important aspect of this finding is the successful allowance for quenching by flame stretch, through the burning probability function p(b). This relates the burning mass fraction to the distribution of flame stretch rates.

NOMENCLATURE

A equivalent flame surface area
$\bar{A}$ dimensionless flame area ($=A_f/L^2$)
a stretch dependency factor
B $=(40.4)^{0.5}(u'/u_l)R_L^{0.5}$
t elapsed time from ignition
$\bar{t}$ dimensionless time ($=tu'/L$)
t' time of entrainment
$\bar{t}'$ dimensionless time ($=t'u'/L$)

c constant
I counter for flame elements
K dimensionless Karlovitz stretch factor ($=u'\varepsilon_l/(\lambda u_l)$)
L integral length scale of turbulence
Le Lewis number
turbulence
l_e size of energy containing eddies
m mass
M dimensionless mass ($=m/\rho_u L^3$)
n number of concentric shells
p(b) probability of undergoing burning
p(s) pdf of s
r equivalent flame radius
ṙ dimensionless radius (=r/L)
R_L turbulent Reynolds number ($=u'L/\nu$)
s stretch rate
$\Delta\bar{t}$ dimensionless time step
(t) value of parameter at t
u burning velocity
u_t fully developed turbulent burning velocity
u' r.m.s turbulent velocity
ϵ relative error
η Kolmogorov scale of
κ dimensionless stretch rate($=s\delta_l/u_l$)
κ' dimensionless stretch rate
λ Taylor micro scale of turbulence
ν kinematic viscosity
ρ gas density
σ_κ dimensionless r.m.s rate of stretch
τ constant of proportionality
τ_a integral time scale (=L/u')
δ flame thickness

subscripts
e entrained; b burnt; u unburnt; qt quench value; l laminar; t turbulent; k effective.

REFERENCES

1. Tennekes, H., *Phys. Fluids*, vol 11 no. 3, 1968, pp 669-671
2. Kuo, Y. and Corrsin, S., *J. Fluid Mech.* vol 50 part 2, 1971, 285-319
3. Kuo, Y. and Corrsin, S., *J. Fluid Mech.* vol 56 part 3, 1972, pp 447-479
4. McCormark, P. D., Scheller, K., Mueller, G. and Tisher, R., *Combust. and Flame,* 19, 1972, pp 297-303
5. Chomiak, J., *16th Symposium on Combustion*, 1977, pp 1665-1673
6. Denashyar, H. and Hill, P. G., *Prog. Energy Combustion sci.* vol 13, 1987, pp 47-73
7. Blizard, N. C., and Keck, C., SAE paper 740191, 1974
8. Tabaczyski, R. J., Trinker, F. H. and Shannon, B.A.S., *Combustion and Flame*, 39, 1980 pp 111-121

9. Abdel-Gayed, R. G., and Bradley, D., *Trans. Am. Soc. Mech. Engrs. J. Fluids Eng,* 99, 1977, pp 732-736
10. Abdel-Gayed, R.G., Bradley, D., and Lawes, M. *Proc. Royal Soc.* A414, 1987, pp 389-413
11. Bradley, D., Lau, A., and Lawes, M., *Proc. Royal Society,* 1992
12. Akindele, O. O., Bradley, D., and MacMahon, M., *Combustion and Flame* 47, 1982 pp 129-155
13. Yeung, P. K., Girimaji, S. S., and Pope, S. B. (1990), *Combustion and flame* **79**, 340-365
14. Law, C. K., Zhu, D. L., and Yu, G., (1988), *21st Symposium on combustion,* 1419-1426
15. Dixon-Lewis, G. (1988), Dynamics of Reactive systems part 1 : Flames 113, *Progress in Astronautics and Aeronautics, Washington: AIAA,* 166-183
16. Taylor, G. I. (1935) *Proc. Royal Society*, **A151** 421-444
17. Abdel-Gayed, R. G., Bradley, D., Lawes, M. and Lung, F. K-K. (1986) 21st Symposium on Combustion pp497-504 (1986)
18. Ziegler, G. F. W., Wagner, E. P., and Maly, R. R. (1985) *20th Symposium on combustion,* 1817-1824
19. Bradley, D., and Lung, F. K-K. (1987) *Combustion and Flame* **69,** 71-93
20. Andrews, G. E., & Bradley, D. (1972) *Combustion and Flame* **12,** 275-278
21. Mushi, E. J., Influence of arc discharge on turbuleent mass burning rate, Uhandisi Journal vol. 18 no. 2, 1994,pp 123-133
22. Mushi, E. M. J., (1992), Ph.D Thesis, University of Leeds (UK)
23 Hurle, I. R., Price, R. B., Sugden, T. M. And Thomas, A. (1968) *Proc. Royal Society London,* **A303** pp 409-427
24. Abdel-Gayed, R. G., Al-Khishali, K. J., and Bradley, D. (1984) *Proc. Royal Society* **A391,** 393-414
25. Al-Khishali, K. J., (1984) PhD Thesis, University of Leeds
26. Habik, S. E. , (1986) PhD Thesis, University of Leeds